
Physicochemical Characterization of Waters in Aquifer AQ2 of the Pointe-Noire Region: Application of Multivariate Statistical Analysis Methods

Frederic Balounta Ngoma¹, Christian Tathy^{1,2,*}, Romain Richard Niere¹, Laurent Matini²

¹Laboratory of Mechanics Energy and Engineering, Higher National Polytechnics School, Marien Ngouabi University, Brazzaville, Congo

²Department of Exact Sciences, Higher Teacher's Training School, Marien Ngouabi University, Brazzaville, Congo

Email address:

frederic.balouta@gmail.com (F. B. Ngoma), tathychristian@yahoo.fr (C. Tathy)

*Corresponding author

To cite this article:

Frederic Balounta Ngoma, Christian Tathy, Romain Richard Niere, Laurent Matini. Physicochemical Characterization of Waters in Aquifer AQ2 of the Pointe-Noire Region: Application of Multivariate Statistical Analysis Methods. *Journal of Water Resources and Ocean Science*. Vol. 11, No. 1, 2022, pp. 1-13. doi: 10.11648/j.wros.20221101.11

Received: January 20, 2022; **Accepted:** February 14, 2022; **Published:** February 25, 2022

Abstract: Located on the Atlantic coast, the city of Pointe-Noire is the economic capital of the Republic of Congo. It enjoys strong industrial activity, particularly oil, with the presence of a refinery and onshore drilling in its surroundings. The steady growth of its population leads to an increase in its drinking water supply needs, produced mainly from the exploitation of its aquifer system. Thus, in view of the growth of its human activities, the interest of permanent monitoring of the quality of its groundwater is becoming more and more great. The present study aims to assess the physicochemical quality of the groundwater in the AQ2 aquifer of the Pointe-Noire region during the period from 2017 to 2020, and to understand the processes that are at the origin of the mineralization of these waters. To this end, we obtained from the water supply company, La Congolaise Des Eaux (LCDE) seventy-five (75) water analysis reports bulletins representing the average values of thirteen (13) physicochemical parameters in each of the 75 boreholes used for this study so as to homogeneously cover the entire city. The Piper diagram revealed that the waters are dominated by three types of facies: K-Na-Cl, Mg-Ca-SO₄-Cl and Mg-Ca-HCO₃. The presence of the K-Na-Cl facies is due to the high levels of chlorides and sodium in the water-rock. The Principal Component Analysis (PCA) indicates that the mineralization of these waters results in the hydrolysis of silicate minerals. The Ascending Hierarchical Classification (AHC) analysis made it possible to determine the parameters that categorize the different classes from 2017 to 2020, these are TDS, EC and TH and to a lesser extent Ca²⁺, Mg²⁺, HCO₃⁻ and TAC. Overall, the quality of the groundwater is good according to standards WHO, but in some cases requires specific treatment before supply.

Keywords: Groundwater, AQ2 Aquifer, Hydrogeochemical Facies, Principal Component Analysis, Ascending Hierarchical Classification

1. Introduction

The Republic of the Congo, like the other countries of Central Africa, is facing water problems in certain localities (such as the Pointe-Noire region). The country is crossed by a large river and also contains significant groundwater [1]. However, there are the problems of controlling the resource and supplying the various consumers in the Pointe-Noire region. Indeed, groundwater (in this region) is subject to multiple constraints due to strong demographic growth and to inadequate or even lack of sanitation. Landfills, cemeteries,

sewage systems, septic tanks, factory sewage as well as solid waste are the main sources of groundwater pollution in the urban sector. According to the drinking water supply company "La Congolaise Des Eaux (LCDE)", the Pointe-Noire region has to day nearly 2000 private boreholes, and observations and surveys of groundwater on the ground indicate overexploitation of the aquifer AQ2 due to the proliferation of boreholes. Despite the importance of the economic and health interests at stake, the functioning of the aquifer in this zone poorly understood and the consequences of uncontrolled exploitation of deep boreholes have not been evaluated [1-6].

It is therefore important to know and control the quality of this resource. The chemical composition of water from the natural environment is very variable. It depends on the geological nature of the soil from which it comes and also on the reactive substances that it might have encountered during the flow [7]. The intensive use of natural resources and the increase in human activities cause serious problems quality of groundwater [8, 9].

This study aims to assess the hydrochemistry quality of the waters of the AQ2 aquifer through private boreholes and those of the LCDE in the Pointe-Noire region. To achieve this objective, we obtained at the LCDE laboratory seventy-five (75) water bulletins representing the average values of thirteen (13) physicochemical parameters in each of the 75 boreholes which are used for this study, so as to homogeneously cover the entire Pointe-Noire, region during the period from 2017 to 2020. The data collected are processed using multivariate statistical methods such as

Principal Component Analysis (PCA), Ascending Hierarchical Classification (AHC) groundwater facies was determined using Piper's diagram.

2. Presentation of the Study Area

2.1. Geographic Location

The Pointe-Noire region is located on the Atlantic coast of Central Africa, at the southwestern end of the Republic of Congo, between meridians 11°30' and 12° East and the parallels 4°30' and 5° South. Its area of approximately 15660 hectares is distributed over a radius of 15 kilometers (figure 1). Presenting a very preponderant geographical position to which it owes its most characteristic features, the studied region is an ideal zone of contact between the ocean and the continent where the effects of marine currents and the oceanic air mass are very characteristic [10, 11].

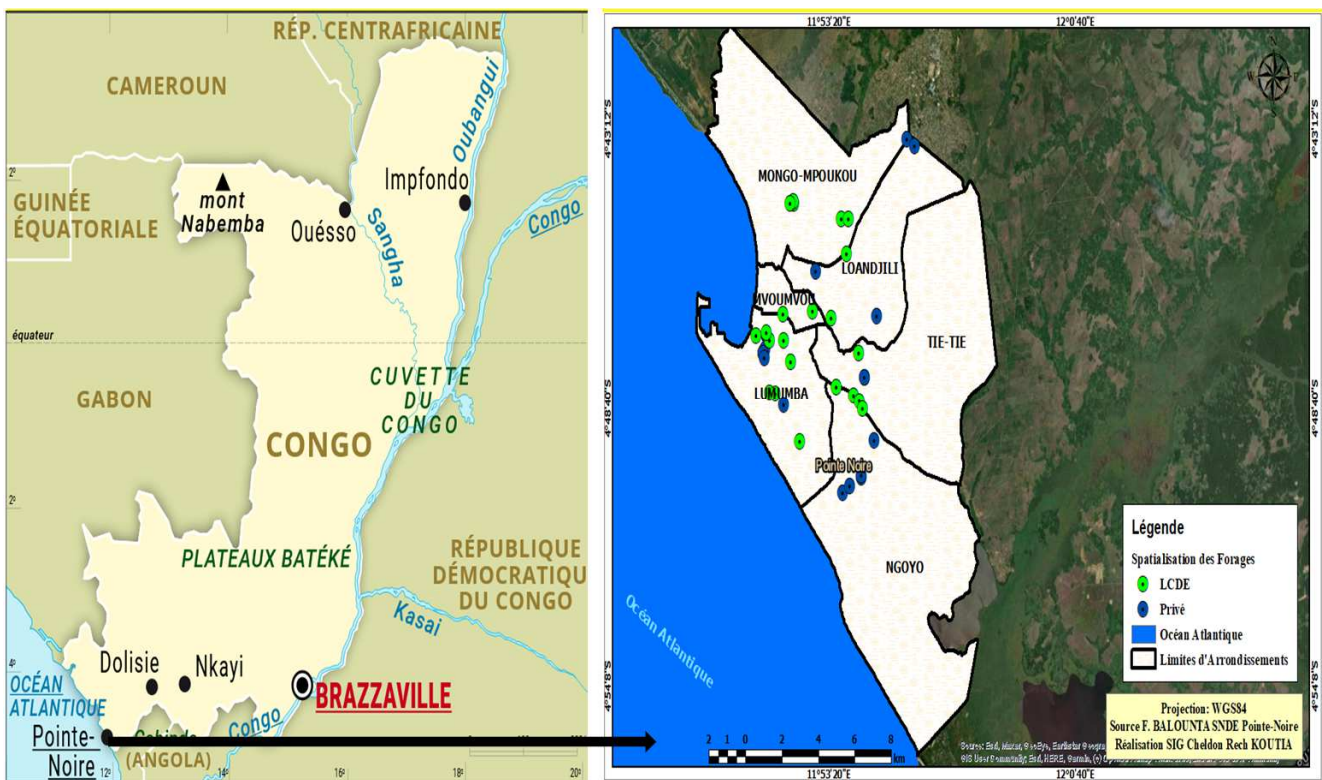


Figure 1. Geographical location boreholes in the study area.

2.2. Climate Context

The study region belongs to the tropical zone. It is also qualified as a zone with an equatorial climate of transition due to the successive influence of the tropical climate and the equatorial climate. The orographic configuration between the seafront and the Mayombe chain exerts an influence on the climate, in particular on precipitation [11-13]. The rainfall regime in the Pointe-Noire region makes it possible to highlight two main annual rainfall periods. These periods are characterized by two seasons:

- 1) a rainy season that begins in October and ends in May, characterized by heavy rains. This period corresponds to groundwater recharge with peaks in february and november;
 - 2) a dry season which is between june and september.
- Precipitation in Pointe-Noire varies at different time scales (that is to say) sometimes the rainy season has the same duration as the dry season [11].

2.3. Geology of the Study Area

The coastal sedimentary basin of Congo is a well-known

region thanks to drilling research for oil, potash and water. This basin is a part of large set of depression delimiting the western edge of the african continent from the Ivory Coast as far as Angola. It corresponds to a zone of subsidence coupled with sedimentary deposits of lake, marine, river and wind origins following a very low monocline structure slope (1%) and resting on the precambrian substratum flush with the Mayombe chain [14]. In the following, only the lithostratigraphic succession of formations necessary for understanding hydrogeology in the study area is described; it concerns the post-salt sedimentary deposits which have been described from numerous oil wells [1, 15]. The soils of the Pointe-Noire region are included in the ferralic arenosols and belonging to the arenosols group is explained by the presence over a depth of more than one meter of a sandy texture, less than 35% by volume of coarse fragments (0% at Pointe-Noire) and the absence diagnostic horizons other than ochric, yermic or albic or an argicou type horizon spodic beyond 50 cm or an argic or spodic type horizon beyond 2 m [16].

2.4. Hydrogeology of the Study Area

Define According to the geological work of oil tankers, and referring to the work of [1, 3, 7], the Pointe-Noire region belongs to the coastal sedimentary basin, and includes an aquifer system composed of several superimposed aquifer layers with hydraulic continuity (figure 2) that can be successively established as follows:

- 1) the free surface aquifer AQ-1 (unconfined) consisting mainly of fine sands with a variable proportion of silts and clays;
- 2) the captive and artesian aquifer AQ-2 (confined) located in the Pointe-Noire region made up of poorly classified sands, sometimes silty, with clayey pastes;
- 3) aquifer AQ-3 (confined) made up of poorly classified conglomeratic sands and with ferruginous concretions;
- 4) aquifer AQ-4 (confined) corresponding to the dolomite unit of the calcaro-dolomitic series identified thanks to the loss of mud from exploration drilling.

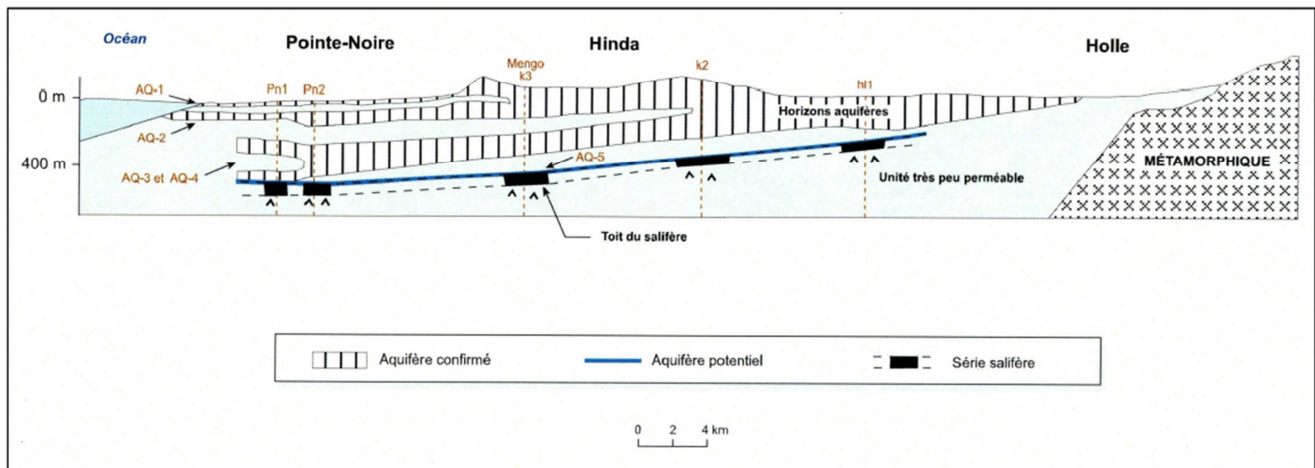


Figure 2. Schematic hydrogeological section of aquifer system of Pointe-Noire [10].

3. Data and Methods

3.1. Sampling

In order to achieve the objective of this study a total of 225 samples of 75 boreholes in the AQ2 aquifer have been collected and analyzed by the laboratory of the drinking water company, LCDE in Pointe-Noire (23 LCDE boreholes and 52 private boreholes). These samples have been collected from 2017 to 2020. Thus, 75 water analysis reports representing the average values of 13 physicochemical parameters in each of the 75 boreholes are used for this study. 14 boreholes are used in the year 2017, 11 boreholes in the year 2018, 37 boreholes in the year 2019 and 13 boreholes in the year 2020.

3.2. Hydrochemical Classification of Water

The chemical parameters in major elements are represented in the Piper diagram which allows a representation of anions and cations on two specific triangles whose sides express the

relative contents (%) of each of the major ions compared to the total of these ions (cations in left triangle and anions in right triangle). The position of a water analysis in these two triangles makes it possible to specify which are the dominant anions and cations. It is important to emphasize that this diagram does not reflect the overall mineralization of water, but only the distribution of dissolved ions. Each borehole has been assigned a label of different color and shape.

3.3. Statistical Analysis

All the data collected on the water of the study region have been subjected to statistical analysis. The multivariate statistic approach was carried out using the normalized principal component analysis (NPCA) and the ascending hierarchical classification (AHC). Statistical analysis was carried out on 75 boreholes and 13 variables: total dissolved solids (TDS), electrical conductivity (EC), temperature $T(^{\circ}C)$, complete alkalimetric content (TAC), total hardness (TH), hydrogen potential (pH) as well as sodium ions Na^{+} , magnesium (Mg^{2+}), potassium (K^{+}), calcium (Ca^{2+}),

chloride (Cl^-), bicarbonate HCO_3^- and sulphate (SO_4^{2-}) using the XLSTAT 2020 software. This analysis makes it possible to synthesize and classify a large number of data in order to extract the main factors which are at the origin of the

simultaneous evolution of variables and their reciprocal relationship [17]. It makes it possible to highlight the similarities between two or more chemical variables during their evolution.

Table 1. Descriptive statistics of the physico chemical parameters of the AQ-2 waters expressed during the period 2017-2020.

Parameter	TDS mg/L	T°C	CE µs/cm	TAC mg/Lcaco ₃	TH mg/Lcaco ₃	pH 6.5-8.5	Ca ²⁺ mg/L	Mg ²⁺ mg/L	Na ⁺ mg/L	K ⁺ mg/L	HCO ₃ ⁻ mg/L	SO ₄ ²⁻ mg/L	Cl ⁻ mg/L	
2017	Min	4	20	8	1	2	7	0	19	5	1	7	32	
	Max	229	25.4	322.16	160	83.6	8	49.94	14.97	24.43	6.25	198.2	9.79	40.28
	Med	47.86	21.64	83.58	18.97	22	7.08	10.98	4.84	20.83	5.34	21.98	7.20	34.7
	SD	59.61	1.74	87.99	42.85	24.66	0.50	13.68	4.79	1.20	0.31	52.55	0.74	1.87
2018	Min	10	20.1	1.21	1.66	10	5.18	3.45	0.69	0.8	0.2	2.02	0.32	1.4
	Max	616	25.6	662	100.6	604.7	7	181.2	36.24	42.28	10.87	122.7	16.91	73.68
	Med	142.2	21.65	173.75	18.3	141.7	6.39	42.52	8.50	10	2.55	22.32	3.96	17.29
	SD	187.9	2.15	215.24	28.21	185.4	0.53	55.54	11.11	12.99	3.33	34.40	5.18	22.58
2019	Min	9	20	19	7.01	9.51	5.7	3.51	1.23	1.33	0.76	8.55	0.93	1.99
	Max	381	29.5	748	353.5	374.4	7.93	112.2	25.98	28	17.66	353.5	19.84	45.6
	Med	89.79	22.27	178.64	70.92	89.40	6.92	30.69	9.27	9.88	5.18	80.97	6.43	15.35
	SD	100.44	3.07	197.15	96.20	98.7	0.66	31.36	8.66	9.28	5.22	100.41	6.30	14.73
2020	Min	8	20	19	2.33	5.006	6.4	2.7	0.6	0.7	0.2	2.83	0.3	1.2
	Max	320	20	640	562.83	320	7.9	123.99	47.19	44.8	28.19	686.66	37.17	67.2
	Med	110.74	20	217.62	139.94	107.87	7.33	37.75	11.74	11.98	6.33	170.76	8.75	18.76
	SD	100.3	0.0	198.11	157.65	99.92	0.60	35.83	13.07	12.37	8	192.34	10.49	18.67
Standards OMS	500 mg/L	25°C	300 µs/cm	- mg/Lcaco ₃	300 mg/Lcaco ₃	6.5-8.5	75 mg/L	30 mg/L	200 mg/L	12 mg/L	300 mg/L	150 mg/L	250 mg/L	

SD: standard deviation; Med: Medium; Max: Maximum; Min: Minimum.

Table 2. Bacteriological parameters of AQ-2 waters in the Pointe-Noire region.

years	parameters	Totals Germs	Total coliforms	Fecal coliforms	Escherichia Coli
		10 UCF/ml	0 UFC/100 ml	0 UFC/100 ml	0 UFC/100 ml
2017	Minimum	60	3	0	0
	Maximum	302	133	100	69
	Median	100	10	0	0
	Average	120.2	32.2	14.7	8.7
	standard deviation	74.8	44.4	31.1	21.4
2018	Minimum	1	0	0	0
	Maximum	100	40	1	0
	Médian	50	0	0	0
	Average	47.6	11	0.25	0
	standard deviation	32.9	17.5	0.5	0
2019	Minimum	7	0	0	0
	Maximum	100	10	1	0
	Médian	56	0	0	0
	Average	48.9	1.2	0.1	0
	standard deviation	25.5	3	0.3	0
2020	Minimum	12	0	0	0
	Maximum	160	10	1	0
	Médian	60	0	0	0
	Average	73.6	2	0.2	0
	standard deviation	65	4.5	0.4	0
	Standards OMS	10 UCF/ml	0 UFC/100 ml	0 UFC/100 ml	UFC/100 ml

3.4. Physicochemical and Bacteriological Data of Borehole Water in the Pointe-Noire Region During the Period 2017-2020

One presents in this section the results of the physicochemical and bacteriological analyzes of the borehole water of the AQ-2 aquifer in the Pointe-Noire region. In fact,

one has obtained 75 water analysis reports for which the descriptive statistics are shown in tables 1 and 2. These tables give the values of the bacteriological and physicochemical parameters of these waters. From these tables, one can conclude according to the standards required by WHO ([18]) that the quality of the analyzed water, is acceptable on the physicochemical point of view (table 1). For all the water bulletins analyzed, the pH value is within the acceptable limits

for drinking water (5.18-8). Poor hygienic conditions on the microbiological level are observed with the presence of total germs, total coliforms which are outside WHO standards (table 2). On the 75 boreholes, 32 boreholes do not comply with hygienic conditions and are infected with germs. The waters of LCDE boreholes (23 boreholes) does not contain germs, these waters are not muddy or cloudy despite the defective distribution network. However, there are puddles of water in some defective piping, favoring the presence of bacteria in the network.

4. Results and Discussion

4.1. Annual Distribution of Cations and Anions in meq/L

The composition relating to a cation or anion is expressed as a percentage of meq/l of the total of the cations or anions (figure 3). The order of predominance of cations and anions expressed as a percentage of meq/l, based on the average calculated over all the holes, is respectively:

for 2017: $\text{Na}^+ > \text{Ca}^{2+} > \text{Mg}^{2+} > \text{K}^+$; $\text{Cl}^- > \text{HCO}_3^- > \text{SO}_4^{2-}$;

for 2018: $\text{Ca}^{2+} > \text{Mg}^{2+} > \text{Na}^+ > \text{K}^+$; $\text{Cl}^- > \text{HCO}_3^- > \text{SO}_4^{2-}$;

for 2019: $\text{Ca}^{2+} > \text{Mg}^{2+} > \text{Na}^+ > \text{K}^+$; $\text{HCO}_3^- > \text{Cl}^- > \text{SO}_4^{2-}$;

for 2020: $\text{Ca}^{2+} > \text{Mg}^{2+} > \text{Na}^+ > \text{K}^+$; $\text{HCO}_3^- > \text{Cl}^- > \text{SO}_4^{2-}$.

From figure 3, one notices in 2017 an excess of $\text{Na}^+ + \text{K}^+$ cations compared with $\text{Ca}^{2+} + \text{Mg}^{2+}$ cations unlike in 2018, 2019 and 2020 where one observes an excess of $\text{Ca}^{2+} + \text{Mg}^{2+}$ cations compared with $\text{Na}^+ + \text{K}^+$ cations.

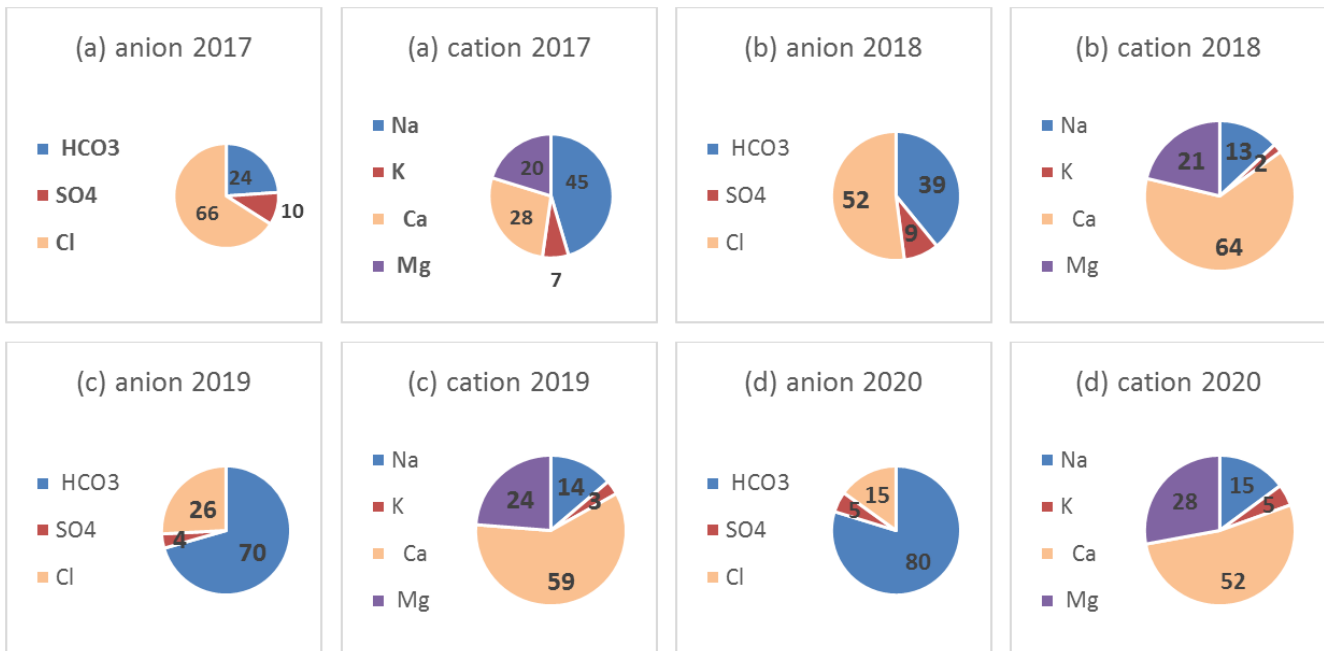


Figure 3. Average composition in % meq/l of major cations and anions in water from AQ2.

4.2. Piper Diagram

The representation of the concentrations of the major elements contents in the Piper diagram (figure 4(a) to 4(d)) obtained using the Diagram software [19], allows to have a global idea of the different types of water encountered in the AQ2 aquifer. Several facies are identified.

For the waters in the year 2017, figure 4(a) presents in general three facies: the K-Na-Cl facies in 8 boreholes (57.15% of the total boreholes) followed by the Mg-Ca-SO₄-Cl facies in 3 boreholes (35.71% of the total boreholes) and finally the Mg-Ca-HCO₃ facies with 1 borehole (7.14% of the total boreholes). Thus, the waters of 2017 (figure 4(a)) are predominantly K-Na-Cl facies. Indeed, by observing the Piper

diagram (figure 4(a)), we see the predominance of Na^+ , Ca^{2+} and Mg^{2+} . The dominant anions are Cl^- .

For the waters in the year 2018, figure 4(b) shows a single Mg-Ca-SO₄-Cl facies within 8 boreholes or 72.73% of the total boreholes. One sees the predominance of Ca^{2+} and Mg^{2+} in two boreholes and no borehole shows dominant cations. The dominant anions are Cl^- , HCO_3^- .

For the waters in the year 2019, figure 4(c) shows two Mg-Ca-HCO₃ facies within 20 boreholes, or 54.05% of the total boreholes followed by the Mg-Ca-SO₄-Cl facies with 3 boreholes, or 8.11% of the total drilling. It can be seen that the Mg-Ca-HCO₃ facies predominate in the 2019 waters (figure 4(c)). However, we observe the predominance of calcium Ca^{2+} . The dominant anions are HCO_3^- .

For the waters in the year 2020, figure 4(d) shows two

Mg-Ca-HCO₃ facies in 10 boreholes, or 76.92% of the total boreholes, followed by the Mg-Ca-SO₄-Cl facies in one borehole either 7.69% of the total drillings. However, we

observe the predominance of calcium Ca²⁺. The dominant anions are HCO₃⁻.

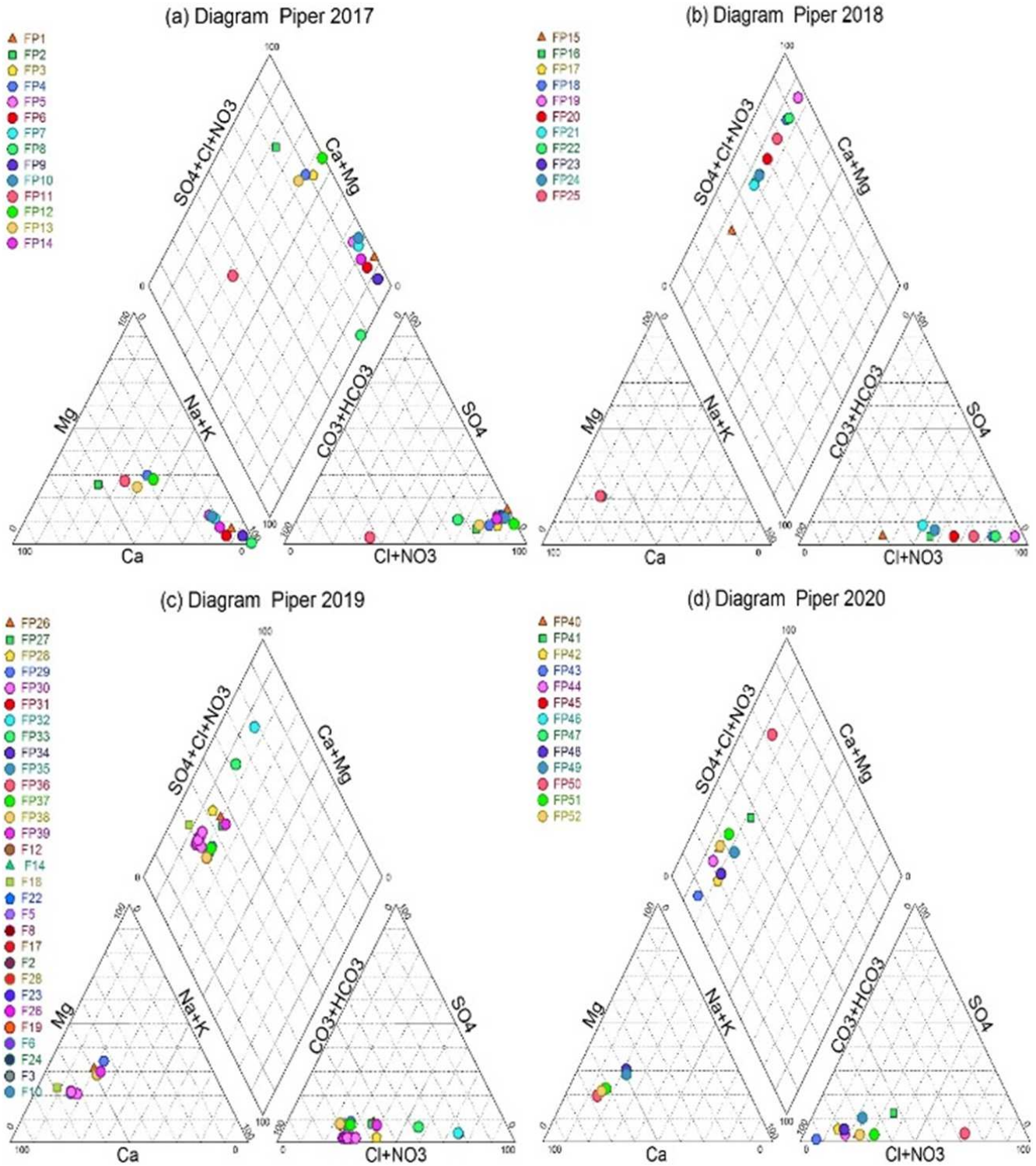


Figure 4. Chemical facies of the waters of the AQ2 boreholes from 2017 to 2020.

4.3. PCA Results for the Years 2017, 2018, 2019 and 2020

Statistical results obtained using PCA are shown in tables 3 to 14, and in figures 5((a) to (d)).

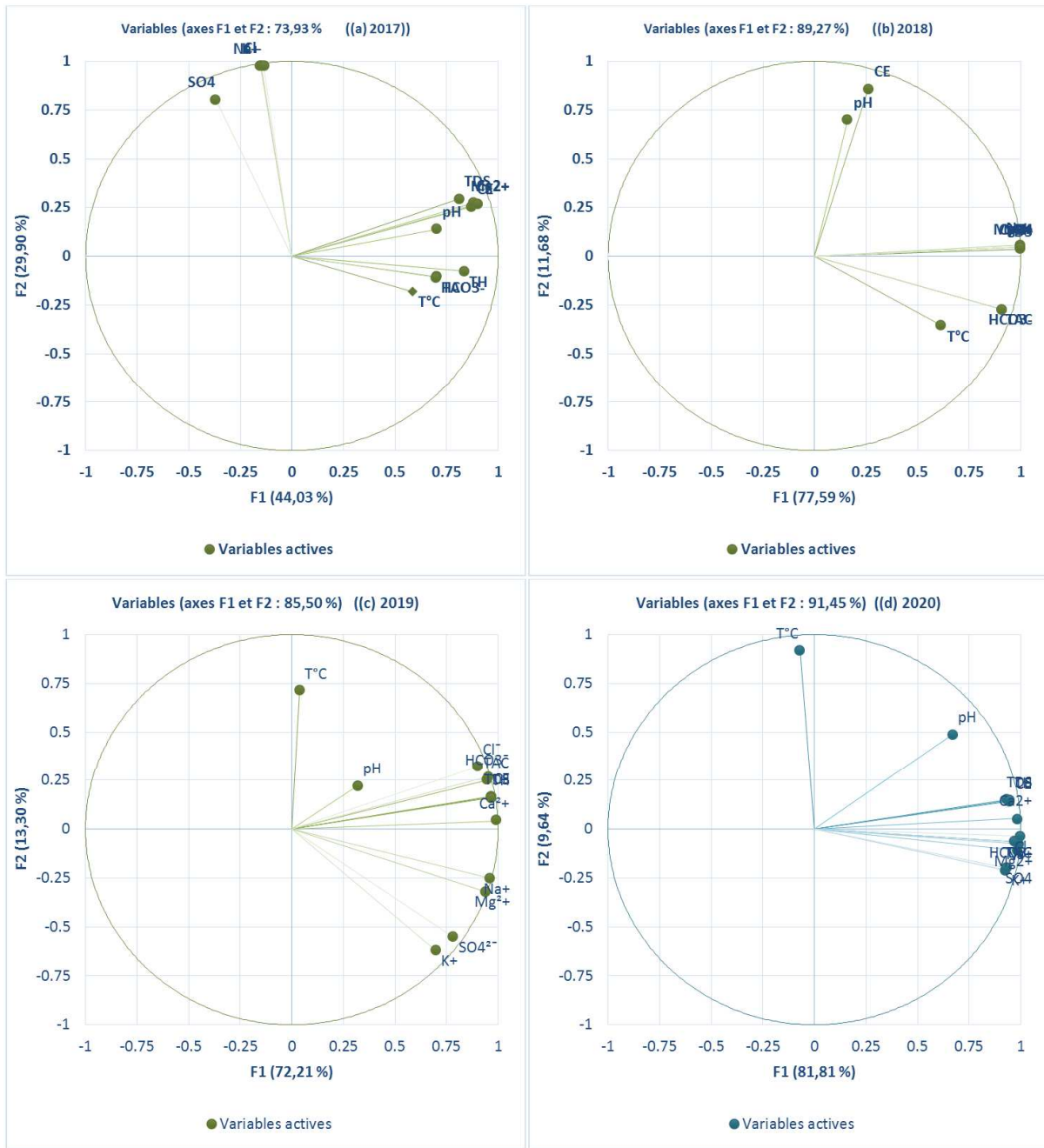


Figure 5. ACP for the years 2017, 2018, 2019 and 2020.

The results of the year 2017 campaign are shown in tables 3; 4 and 5 as well as in figure 5(a). Table 3 shows the eigenvalues and the variances for each variable. Factor F1, with variance of 44.03%, is the most important of all, followed by factor F2, with 29.9% of variance. These two factors reflect most of the information sought and make it possible to represent the cloud of points in a significant way because the cumulative variance of these factors is 73.93%.

Table 3. Eigenvalues for the year 2017.

	F1	F2
Eigenvalue	5.72	3.89
Total variance (%)	44.03	29.90
Cumulative (%) of variance	44.03	73.93

Table 4. Correlation between variables and factors for the year 2017.

	F1	F2
TDS	0.81	0.30
T°C	0.58	-0.18
EC	0.87	0.25
TAC	0.70	-0.11
TH	0.84	-0.08
pH	0.70	0.14
Ca ²⁺	0.88	0.27
Mg ²⁺	0.90	0.27
Na ⁺	-0.15	0.97
K ⁺	-0.15	0.98
HCO ₃ ⁻	0,0	-0.11
SO ₄ ²⁻	-0.37	0.80
Cl ⁻	-0.14	0.98

Table 4 gives coefficients of correlation which explain the contribution of the different variables in the definition of the main factors. Thus, each factor is defined by a number of essential variables in the mechanism of water mineralization. This table shows that the most important factor F1 is defined by TDS ($r=0.81$), EC ($r=0.87$), TAC ($r=0.7$), TH ($r=0.84$), pH ($r=0.7$), Ca^{2+} ($r=0.88$), Mg^{2+} ($r=0.9$) and HCO_3^- ($r=0.69$). The factor F2 is defined by sodium Na^+ ($r=0.97$), K^+ ($r=0.97$), SO_4^{2-} ($r=0.8$) and Cl^- ($r=0.97$).

Table 5 reveals weak and negative, weak, strong and positive correlations between variables. Thus, the pH ($r=0.59$), Ca^{2+} ($r=0.98$), Mg^{2+} ($r=0.95$) shows a strong correlation with EC. There is a strong correlation between Ca^{2+} ($r=0.6$), Mg^{2+} ($r=0.73$) and pH. In addition, there is also a strong correlation between Ca^{2+} and Mg^{2+} ($r=0.94$), Na^+ and K^+ ($r=1$), Na^+ and SO_4^{2-} ($r=0.86$), Na^+ and Cl^- ($r=1$), K^+ and Cl^- ($r=1$), K^+ and SO_4^{2-} ($r=0.86$), Cl^- and SO_4^{2-} ($r=0.86$).

There are also negative correlations between variables with very low values (table 5). Based on the critical correlation coefficient $r = 0.64$ [20], sodium and potassium are strongly correlated with chloride ($r=1$), which explains the presence of salt in groundwater. The space of the variables of the factorial design F1-F2 (figure 5(a)) shows that this design expresses 73.93% of the cumulative variance. The elements which define the factor F1 (44.03%) come from a considerable duration of due to following water-rock contact. These elements come from the hydrolysis of silicate minerals present in the rocks which constitute the bedrock of the aquifers that shelter the waters of this multilayer system [4]. Indeed, hydrolysis being a slow process, the factor F1 accounts for the conditions of acquisition of water composition chemism. The factor F2 (29.9%) highlights the underground exchanges between the waters of this environment and the waters of the ocean.

Table 5. Correlation matrix (Pearson (n)) for the year 2017.

Variables	TDS	T°C	EC	TAC	TH	pH	Ca^{2+}	Mg^{2+}	Na^+	K^+	HCO_3^-	SO_4^{2-}	Cl^-
TDS	1												
T°C	0.21	1											
EC	0.98	0.29	1										
TAC	0.28	0.61	0.36	1									
TH	0.43	0.76	0.54	0.76	1								
pH	0.55	0.18	0.59	0.37	0.55	1							
Ca^{2+}	0.98	0.34	0.98	0.39	0.56	0.60	1						
Mg^{2+}	0.91	0.32	0.95	0.42	0.68	0.73	0.94	1					
Na^+	0.09	-0.18	0.06	-0.13	-0.15	0.03	0.08	0.09	1				
K^+	0.10	-0.18	0.06	-0.13	-0.15	0.03	0.08	0.09	1	1			
HCO_3^-	0.27	0.61	0.36	1.00	0.76	0.36	0.39	0.41	-0.13	-0.13	1		
SO_4^{2-}	-0.20	-0.17	-0.23	-0.12	-0.20	-0.27	-0.19	-0.22	0.86	0.86	-0.12	1	
Cl^-	0.11	-0.18	0.08	-0.13	-0.15	0.04	0.10	0.11	1	1	-0.13	0.86	1

Table 6. Eigenvalues for the year 2018.

	F1	F2
Eigenvalue	10.09	1.52
Total variance (%)	77.59	11.68
Cumulative (%) of variance	77.59	89.27

Table 7. Correlation between variables and factors for the year 2018.

	F1	F2
TDS	0.998	0.036
T°C	0.616	-0.356
EC	0.262	0.859
TAC	0.911	-0.272
TH	0.997	0.047
pH	0.162	0.698
Ca^{2+}	0.997	0.047
Mg^{2+}	0.997	0.047
Na^+	0.996	0.057
K^+	0.997	0.048
HCO_3^-	0.911	-0.272
SO_4^{2-}	0.997	0.048
Cl^-	0.997	0.047

The results of the PCA in 2018 are presented in tables 6; 7 and 8 as well as in figure 5(b). The analysis of these results makes it possible to observe the eigenvalues and the variances for each factor as well as the cumulative variances (table 6). The analysis of the factorial plane F1-F2 (figure 5(b))

highlights the general trends. Indeed, the factor F1 has a variance of 77.59%, the most important. Then comes the factor F2 with 11.68% of variance. The cumulative variance is 89.27% for the two factors (table 6).

Table 7 gives the contribution of the different variables in the definition of the main factors. This table shows that the factor F1, is defined by TDS ($r=0.99$), T°C ($r=0.62$), TAC ($r=0.91$), TH ($r=0.99$), Ca^{2+} ($r=0.99$), Mg^{2+} ($r=0.99$) and HCO_3^- ($r=0.91$), K^+ ($r=0.99$), Na^+ ($r=0.99$), SO_4^{2-} ($r=0.99$) and Cl^- ($r=0.99$). The factor F2 is defined by EC ($r = 0.86$), pH ($r = 0.69$).

The relationship link between all variables and coefficients of correlation between these different variables are given by the correlation matrix (table 8). Table 8 shows that TDS is strongly correlated with the following variables TH ($r=1$), Ca^{2+} ($r=1$), Mg^{2+} ($r=1$), Na^+ ($r=1$), K^+ ($r=1$), HCO_3^- ($r=0.89$), SO_4^{2-} ($r=1$) and Cl^- ($r=1$). Hardness (TH) is strongly correlated with the following elements: Ca^{2+} ($r=1$), Mg^{2+} ($r=1$), Na^+ ($r=1$), K^+ ($r=1$), HCO_3^- ($r=0.88$), SO_4^{2-} ($r=1$), K^+ ($r=1$). Based on the critical correlation coefficient $r=0,64$ [7], we can note a strong correlation between Na^+ and Cl^- ($r=1$), K^+ and Cl^- ($r=1$), Ca^{2+} and Mg^{2+} ($r=1$), Ca^{2+} and Na^+ ($r=1$), Ca^{2+} and K^+ ($r=1$), Ca^{2+} and HCO_3^- ($r=0.88$), Ca^{2+} and SO_4^{2-} ($r=1$), Ca^{2+} and Cl^- ($r=1$). The strong correlation between Na^+ and Cl^- ($r=1$), K^+ and Cl^- ($r=1$) shows the likely saline intrusion into groundwater in the

Pointe-Noire region. This principal component analysis applied to groundwater of the aquifer AQ2 allows one to say that the mineralization of groundwater is controlled by anthropogenic and possible atmospheric. AQ2 aquifer, where ionic exchanges, alteration of primary minerals or dissolution

of secondary minerals, seem to play an insignificant role in the mineralization of groundwater [4]. Calcium, magnesium and bicarbonates could, in this context, be the best indicators of water-rock interaction.

Table 8. Correlation matrix (Pearson (n)) for the year 2018.

Variables	TDS	T°C	EC	TAC	TH	pH	Ca ²⁺	Mg ²⁺	Na ⁺	K ⁺	HCO ₃ ⁻	SO ₄ ²⁻	Cl ⁻
TDS	1												
T°C	0.59	1											
EC	0.31	0.02	1										
TAC	0.89	0.52	0.12	1									
TH	1	0.59	0.32	0.88	1								
pH	0.15	0.15	0.36	0.12	0.16	1							
Ca ²⁺	1	0.59	0.32	0.88	1	0.16	1						
Mg ²⁺	1	0.59	0.32	0.88	1	0.16	1	1					
Na ⁺	1	0.58	0.33	0.88	1	0.16	1	1	1				
K ⁺	1	0.59	0.32	0.88	1	0.16	1	1	1	1			
HCO ₃ ⁻	0.89	0.52	0.12	1	0.88	0.16	0.88	0.88	0.88	0.88	1		
SO ₄ ²⁻	1	0.59	0.32	0.88	1	0.16	1	1	1	1	0.88	1	
Cl ⁻	1	0.59	0.32	0.88	1	0.16	1	1	1	1	0.88	1	1

Table 9. Eigenvalues for the year 2019.

	F1	F2	F3
Eigenvalue	9.39	1.73	1.20
Total variance (%)	72.21	13.30	9.26
Cumulative (%) of variance	72.21	85.50	94.76

Table 10. Correlation between variables and factors for the year 2019.

	F1	F2	F3
TDS	0.97	0.16	-0.18
T°C	0.04	0.71	0.50
EC	0.97	0.17	-0.17
TAC	0.95	0.25	-0.16
TH	0.97	0.16	-0.17
pH	0.32	0.22	0.80
Ca ²⁺	0.99	0.04	-0.11
Mg ²⁺	0.94	-0.32	0.10
Na ⁺	0.96	-0.25	0.07
K ⁺	0.69	-0.62	0.31
HCO ₃ ⁻	0.95	0.27	-0.10
SO ₄ ²⁻	0.78	-0.55	0.24
Cl ⁻	0.90	0.32	0.01

The PCA results for the year 2019 are presented in tables 9, 10 and 11 as well as in figure 5(c). The analysis of these results makes it possible to observe the eigenvalues and the variances expressed for each factor as well as the cumulative variances (table 9). The analysis of the factorial plane F1-F2 (figure 5(c)) highlights the general trends. Indeed, the factor F1, has a variance of 72.21%, the most important of all, then come the factors F2 and F3, with respectively 13.30% and 9.26% of the variance. These three factors reflect most of the information sought and make it possible to represent the scatter plot significantly because the cumulative variance of these factors is 94.76%.

The contribution of the different variables in the definition of the main factors is given in Table 10. This table shows that the most important factor F1 is defined by TDS (r=0.97), CE (r=0.97), TAC (r=0.95), TH (r=0.97), Ca²⁺ (r=0.99), Mg²⁺ (r=0.94) and HCO₃⁻ (r=0.95), Na⁺ (r=0.96), and Cl⁻ (r=0.89). The ions K⁺ (r=0.69), SO₄²⁻ (r=0.78) are correlated with factor F1 with a lesser degree. Factor F2 is defined by T (°C) (r = 0.71) and factor F3 is defined by pH (r = 0.80).

Table 11. Correlation matrix (Pearson (n)) for the year 2019.

Variables	TDS	T°C	EC	TAC	TH	pH	Ca ²⁺	Mg ²⁺	Na ⁺	K ⁺	HCO ₃ ⁻	SO ₄ ²⁻	Cl ⁻
TDS	1												
T°C	0.04	1											
EC	1.00	0.05	1										
TAC	0.98	0.14	0.98	1									
TH	1.00	0.05	1.00	0.98	1								
pH	0.23	0.35	0.23	0.23	0.23	1							
Ca ²⁺	0.99	0.01	0.99	0.97	0.99	0.25	1						
Mg ²⁺	0.83	-0.10	0.83	0.79	0.83	0.28	0.90	1					
Na ⁺	0.87	-0.08	0.87	0.84	0.87	0.28	0.93	0.99	1				
K ⁺	0.50	-0.19	0.50	0.46	0.51	0.27	0.62	0.89	0.84	1			
HCO ₃ ⁻	0.97	0.17	0.97	0.99	0.97	0.28	0.96	0.79	0.83	0.47	1		
SO ₄ ²⁻	0.61	-0.18	0.61	0.57	0.62	0.26	0.72	0.95	0.91	0.97	0.57	1	
Cl ⁻	0.90	0.21	0.91	0.92	0.90	0.39	0.89	0.73	0.77	0.42	0.96	0.52	1

Significant links existing between the various parameters are given by the correlation matrix (table 11). Based on the critical correlation coefficient $r = 0.64$ [20], EC is strongly correlated with TH ($r = 1$). Note that EC describes inorganic salts present in solution in water. As for the total hardness (TH) of water, it is mainly related to the amount of Ca^{2+} and Mg^{2+} (table 11). Thus, EC has on the one hand a strong correlation with the anions Ca^{2+} ($r=0.98$), Mg^{2+} ($r=0.83$), Na^+ ($r=0.87$) and on the other hand with HCO_3^- ($r=0.97$), Cl^- ($r=0.91$). The elements which define the factor F1 come from a long duration of dissolution due to the water-rock contact. Its elements come from the hydrolysis of minerals present in the bedrock of the aquifers. Hydrolysis being a slow process, the factor F1 therefore expresses the phenomenon of mineralization residence time. The grouping of the majority of variables supported by mineralization around this axis shows the influence of hydrolysis alteration in the dissolution of ions.

Table 12. Eigenvalues for the year 2020.

	F1	F2
Eigenvalue	10.63	1.25
Total variance (%)	81.81	9.64
Cumulative (%) of variance	81.81	91.45

The PCA results for the year 2020 are shown in tables 12, 13 and 14 and in figure 5(d). The analysis of these results also makes it possible to observe the eigenvalues and the variances for each factor as well as the cumulative variance (table 12). The analysis of the factorial plane F1-F2 (figure 5(d)) highlights the general trends. The factor F1, has a variance of 81.81%, then comes the factor F2 with 9.64% of variance. These two factors reflect most of the information sought and make it possible to represent the cloud of points in a significant way because the cumulative

variance of these factors is 91.45%.

The contribution of the different variables in the definition of the main factors is given in table 13. This table shows that the most important factor F1 is defined by TDS ($r=0.93$), EC ($r=0.94$), TAC ($r=0.97$), TH ($r=0.94$), pH ($r=0.67$), Ca^{2+} ($r=0.99$), Mg^{2+} ($r=0.98$), HCO_3^- ($r=0.97$), Na^+ ($r=0.99$), Cl^- ($r=0.99$), K^+ ($r=0.93$) and SO_4^{2-} ($r=0.93$). The factor F2 is defined by temperature $T^{\circ}C$ ($r=0.92$).

Table 13. Correlation between variables and factors for the year 2020.

	F1	F2
TDS	0.93	0.15
$T^{\circ}C$	-0.07	0.92
EC	0.94	0.14
TAC	0.97	-0.07
TH	0.94	0.14
pH	0.67	0.49
Ca^{2+}	0.99	0.05
Mg^{2+}	0.98	-0.11
Na^+	0.99	-0.08
K^+	0.93	-0.21
HCO_3^-	0.97	-0.07
SO_4^{2-}	0.93	-0.20
Cl^-	1	-0.04

Significant links existing between the various parameters are given by the correlation matrix (table 14). These links reflect the different correlations that exist between the variables studied. Based on the critical correlation coefficient $r=0.64$ [20], EC is strongly correlated with TH ($r = 1$). On the one hand, the EC shows a correlation with the ions Ca^{2+} ($r=0.98$), Mg^{2+} ($r=0.87$), Na^+ ($r=0.91$), K^+ ($r=0.76$) and on the other hand with HCO_3^- ($r=0.87$), Cl^- ($r=0.93$), SO_4^{2-} ($r=0.77$). The ions SO_4^{2-} have a good correlation with TH ($r=0.78$). This shows that the SO_4^{2-} ions would come from gypsum formation [2, 21].

Table 14. Correlation matrix (Pearson (n)) for the year 2020.

Variables	TDS	$T^{\circ}C$	EC	TAC	TH	pH	Ca^{2+}	Mg^{2+}	Na^+	K^+	HCO_3^-	SO_4^{2-}	Cl^-
TDS	1												
$T^{\circ}C$	0	1											
EC	1.00	0	1										
TAC	0.85	-0.11	0.87	1									
TH	1	0.01	1	0.87	1								
pH	0.65	0.26	0.64	0.64	0.64	1							
Ca^{2+}	0.98	-0.04	0.98	0.93	0.98	0.64	1						
Mg^{2+}	0.86	-0.12	0.88	0.97	0.88	0.59	0.95	1					
Na^+	0.89	-0.10	0.91	0.96	0.91	0.61	0.97	1	1				
K^+	0.74	-0.16	0.76	0.93	0.76	0.52	0.86	0.98	0.96	1			
HCO_3^-	0.85	-0.11	0.87	1	0.87	0.64	0.93	0.97	0.96	0.93	1		
SO_4^{2-}	0.76	-0.16	0.78	0.93	0.78	0.54	0.88	0.98	0.97	1	0.92	1	
Cl^-	0.92	-0.09	0.94	0.96	0.94	0.62	0.98	0.99	1	0.94	0.96	0.95	1

4.4. AHC for the Years 2017, 2018, 2019 and 2020

The results obtained using AHC are shown in figure 6((a) to (d)) and figure 7((a) to (d)). The 2017 campaign results are reported in figures 6(a) and 7(a), 2018 results are reported in

figures 6(b) and 7(b), 2019 results are reported in figures 6(c) and 7(c) finally the results for 2020 are shown in figures 6(d) and 7(d). Except the year 2018 which have 3 classes the years 2017, 2019 and 2020 have 2 classes.

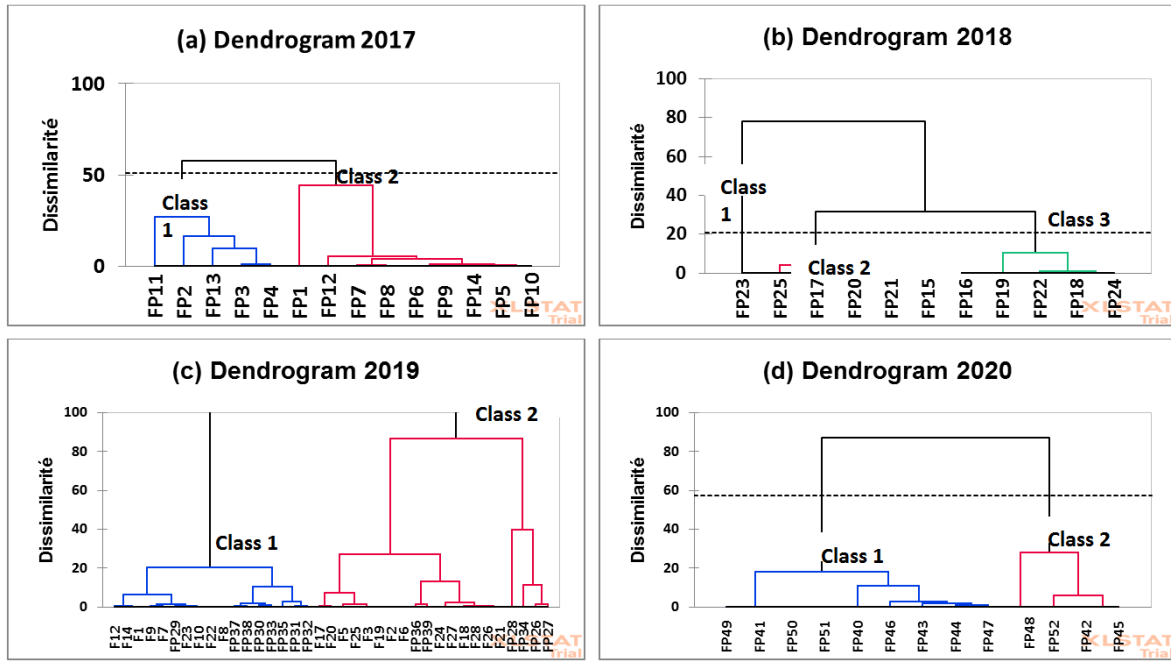


Figure 6. Dendrograms for the years 2017, 2018, 2019 and 2020.

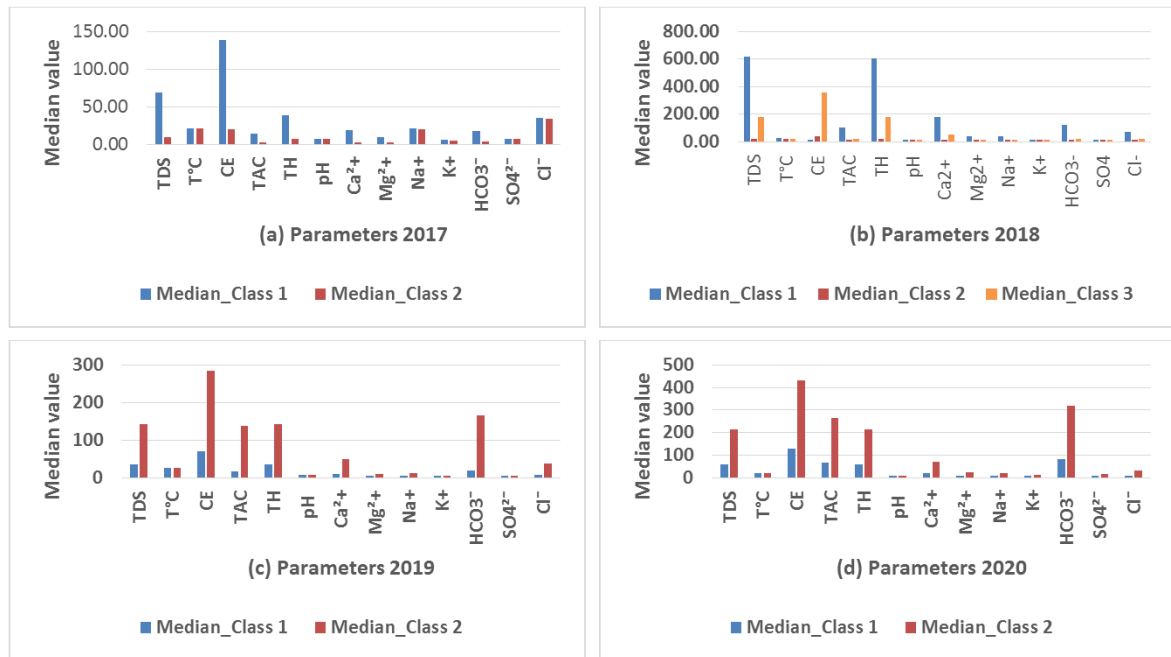


Figure 7. Median values of the 13 physicochemical parameters.

Analyzes of groundwater in Pointe-Noire region show that these waters are weakly mineralized, with an EC average of 180.5 $\mu\text{S}/\text{cm}$ (2017 to 2020). However, its present a respectively low and medium mineralization with the exception of a few boreholes. The waters are acidic, with a pH which varies from 5.18 to 8, with an average of 7 from 2017 to 2020. This average of pH is in agreement with that obtained by [4] which is 6.51 on the waters subsurface of the sedimentary basin of Congo. The acidity of the waters is one of the characteristic features of the waters of the Pointe-Noire region. It would be linked either to the presence in high

quantity of CO_2 in the soil. This acidity comes mainly from the decomposition of organic matter, with the production of CO_2 in the first layers of the soil [22]. The groundwater temperatures of the AQ2 groundwater vary between 20°C and 29.5°C. With an average of 23°C between 2017 and 2020.

Excessive pumping in order to satisfy different uses is the basis of the saline and brackish water intrusion into the groundwater. This phenomenon is highlighted by multivariate analysis (PCA) which reveals the very high correlation between chloride and sodium in AQ2 waters from 2017 to 2020. This event is further justified by the high levels of

chlorides and sodium in waters, hence the chlorinated facies found in most of the groundwaters of the Pointe-Noire region. The Piper diagrams show that these waters are dominated by three types of facies: K-Na-Cl, Mg-Ca-SO₄-Cl and finally Mg-Ca-HCO₃. These results are consistent with those found in [2] (two main chemical facies dominate the waters of AQ2: K-Na-HCO₃ (36.36%) and Mg-Ca-HCO₃ (27.27%)) and in [6] (Who obtained three facies: Mg-Ca-SO₄-Cl, Mg-Ca-HCO₃ and K-Na-HCO₃). The presence of the K-Na-Cl facies is due to the high levels of chlorides and sodium or following water-rock contact. The dominant cations in the waters of AQ2 are Ca²⁺, Na⁺ and Mg²⁺ and the dominant anions are: Cl⁻ and HCO₃⁻.

The different dendrograms (figure 6(a) to (d)) resulting from the ascending hierarchical classification (AHC) highlight several main classes of boreholes.

In the year 2017, one obtains two classes thus, the class 1 composed of five boreholes, is linked to the other class 2 composed of 9 boreholes at a high distance (100). On the other hand, in class 2018 one obtains three classes. The class 1 composed of one borehole, and class 2 composed of six boreholes are linked to class 3 composed of four boreholes at a high distance (100).

In the year 2019, two classes are obtained. The class 1 consisting of seventeen boreholes is linked to class 2 consisting of twenty boreholes at a high distance (100).

In the year 2020 one obtains two classes, class 1 composed of nine boreholes is linked to class 2 composed of four boreholes at a high distance (100). These results indicate that boreholes are geochemically distincts from one to another. To describe the characteristics of each class of boreholes, figure 7((a) to (d)) presents the median values of the 13 physicochemical parameters used in the ascending hierarchical classification from 2017 to 2020. The parameters that categorize all classes from 2017 to 2020 are: TDS, EC, TAC and TH, and to a lesser extent, the Ca²⁺, Mg²⁺, HCO₃⁻. The EC and TDS parameters represent the mineralization of these waters. Descriptive statistics indicate that all classes of each year are geochemically distinct.

5. Conclusion

The study of the hydrochemical characteristics of water resources in the Pointe-Noire region is carried out using the methods of multivariate statistical analysis. This study highlights the different physicochemical characteristics of the waters of this region. From a physical point of view, the temperature of these waters varies between 20 and 29.5°C, pH varies between 5.18 and 8 pH units, which indicates that these waters are acidic. Classification of the results of chemical analyzes obtained from the triangular Piper diagram identifies three groups of water: K-Na-Cl waters, Mg-Ca-SO₄-Cl waters and Mg-Ca-HCO₃ waters. Indeed, the dominant cations in the waters of Pointe-Noire are Ca²⁺, Na⁺ and Mg²⁺ and the dominant anions are: Cl⁻ and HCO₃⁻.

The Principal Component Analysis indicates that the mineralization of these waters is controlled by the phenomenon of mineralization-residence time or hydrolysis of

groundwater. Thus, the strong correlation between Na⁺ and Cl⁻ (r=1), K⁺ and Cl⁻ (r=1) shows the phenomenon of saline intrusion into groundwater in the Pointe-Noire region. On the other hand, the Ascending Hierarchical Classification makes it possible to highlight the parameters that categorize all the classes from 2017 to 2020 (TDS, EC, TAC and TH, and to a lesser extent the Ca²⁺, Mg²⁺, HCO₃⁻). Descriptive statistics indicate that all classes of each year are geochemically distinct groups of samples.

This work completes several previous studies [1-6, 23] providing a database for monitoring the physicochemical and bacterial quality of groundwater in the Pointe-Noire region. However, they deserve to be supplemented by other investigations, in particular studies of the chemical parameters of pollution, heavy metals as well as pesticides.

References

- [1] Moukolo N., (1992). Hydrogéologie du Congo. [Hydrogeology of Republic of the Congo]. Document du BRGM, No 210, éd. BRGM, Orléans, 128p.
- [2] Tathy C, Matini L., Mabilia B., Antoine F and Moukandi-Nkaya G., (2010). Hydrochemistry of groundwater in the aquifer AQ-2 in Pointe-Noire, south west Congo-Brazzaville. Research Journal of Applied Sciences, 5, 361-369. <http://dx.doi.org/10.3923/rjasci.2010.361.369>
- [3] Moukandi-N'kaya G. D., (2012). Etude hydrogéologique, hydrochimique in situ et modélisation hydrodynamique du système aquifère du bassin sédimentaire de la région de Pointe-Noire. [Hydrogeological and hydrochemical in situ study and hydrodynamic modeling of the aquifer system of the sedimentary basin of the Pointe-Noire region]. Thèse de doctorat. Université Marien Ngouabi, Congo- Brazzaville, 132 p.
- [4] Mbilou U. G., Tchoumou M., Ngouala M. M., and Balounguidi J., (2016). Caractérisation hydrogéochimique et microbiologique des eaux souterraines dans le système d'aquifères multi couche de la région de pointe-noire en république du Congo. [Hydrogeochemical and microbiological characterization of groundwater in the multilayer aquifer system of the Pointe-Noire region in the Republic of Congo]. Larhyss Journal, n°28, 257-273.
- [5] Essouli O. F., Boudzoumou F., Miyouna T., Kashala E and Fayes S., (2019). Control and monitoring of the realization of three water boreholes in the congolese coastal sedimentary basin. Larhyss Journal, n°39, 153-180.
- [6] Ngouala M., (2020). Caractérisation hydrochimique des eaux souterraines de la zone de contact du bassin sédimentaire côtier et du socle du Précambrien inférieur au sud-ouest de la République du Congo. [Hydrochemical characterization of groundwater in the contact zone of the coastal sedimentary basin and the lower Precambrian basement in the south-west of the Republic of Congo]. Cinq continents, Revue Roumaine de Géographie, 10 (21), 60-85.
- [7] Nkounkou Tomodiatounga D., (2017). Modélisation hydrodynamique et hydrochimique de l'aquifère 1 de la région de Pointe-Noire. [Hydrodynamic and hydrochemical modeling of aquifer 1 in the Pointe-Noire region]. Thèse de doctorat, université Marien Ngouabi, 108 p.

- [8] Foster S. S. D., (1995). Groundwater for development –an overview of quality constraints. In H. Nash & G. J. H. Mc Call (Eds.), *Groundwater quality*. 17 the Special Report, London United: Chapman and Hall, 1-3.
- [9] Mor S., Ravindra K., Dahiya R. P and Chandra A., (2006). Leachate characterization and assessment of groundwater pollution near municipal solid waste landfill site. *Environ Monit Assess*, n°118, 435-456.
- [10] Suchel J. R., (1972). Répartition des pluies et des régimes pluviométriques au Cameroun. [Distribution of rainfall and rainfall patterns in Cameroun]. GECET et CNRS, n°5, Yaoundé, 287 p.
- [11] Samba-Kimbata M. J., (1991). Précipitations et bilans de l'eau dans le bassin forestier du Congo et ses marges. [Precipitation and water budgets in the Congo forest basin and its margins]. Thèse de doctorat d'état, Univ. Bourgogne, Dijon, 241 p.
- [12] Samba-kimbata M. J., (1978). Le climat du Bas Congo. [The climate of Bas Congo]. Thèse 3eme cycle, Univ. Bourgogne, Dijon, 280 p.
- [13] Peyrot B., (1983). Interprétation géomorphologie du littoral et de la façade maritime atlantique de la république populaire du Congo. [Geomorphological interpretation of the coastline and the Atlantic seaboard of the People's Republic of Congo]. In *Travaux et documents de géographie Tropicale; CECET n°49*, 75-98.
- [14] Sitou L., Tchikaya J., (1991). L'érosion en cirques dans la région côtière du Congo. [Erosion in cirques in the coastal region of the Congo]. *Bulletin de la société géographique de Liège*, 27, 77-91.
- [15] Vernet R., Assoua-Wande C., Massamba L., and Sorriaux P., (1996). Paléogéographie du Crétacé Albien-Maastrichtien du bassin côtier congolais. *Géologie de l'Afrique et de l'Atlantique sud*. [Paleogeography of the Albian-Maastrichtian Cretaceous of the congolese coastal basin. *Geology of Africa and the South Atlantic*]. Actes colloques Angers 1994, 39-55.
- [16] Laclau J. P., (2001). Dynamique du fonctionnement minéral d'une plantation d'eucalyptus. Effets du reboisement sur un sol de savane du littoral congolais; conséquence pour la gestion des plantations industrielles. [Dynamics of the mineral functioning of a eucalyptus plantation. Effects of reforestation on savanna soil of the congolese coast; consequence for the management of industrial plantations]. Thèse de doctorat. INA-PG, 146 p.
- [17] Biemi J., (1992). Contribution à l'étude géologique, hydrogéologique et par télédétection des bassins versants Subsahariens du socle précambrien d'Afrique de l'Ouest. Hydro structurale, hydrochimie et isotopie des aquifères discontinus des sillons et aires granitiques de la Haute Marahoué (Côte d'Ivoire). [Contribution to the geological, hydrogeological and remote sensing study of the Sub-Saharan watersheds of the Precambrian basement of West Africa. Hydrostructural, hydrochemistry and isotopy of discontinuous aquifers in furrows and granitic areas of Haute Marahoué (Ivory Coast)]. Thèse de doctorat d'Etat, Université Nationale de Côte d'Ivoire, 479 p.
- [18] WHO, (2011). Guidelines for drinking water quality, health criteria and other supporting information. 2ème Edn., vol 2, world health organization, Geneva, 231-233.
- [19] Simler R., (2004). Diagrammes. Logiciel d'hydrochimie multilingage en distribution libre. [Diagrams. Multi-language software of hydrochemistry in free distribution]. Laboratoire d'Hydrogéologie d'Avignon, Université d'Avignon.
- [20] Mangin A., (1974). Contribution à l'étude hydrodynamique des aquifères karstiques. Concepts méthodologiques adoptés. Systèmes karstiques étudiés. [Contribution to the hydrodynamic study of karstic aquifers. Methodological concepts adopted. Karst systems studied]. *Ann. Spéléol.*, 29 (4), 495-601.
- [21] Amadou H., Mahaman S., and Abdou M., (2014). Caractérisation hydrochimique des eaux souterraines de la région de Tahoua, Niger. [Hydrochemical characterization of groundwater in the Tahoua region, Niger]. *Journal of Applied Biosciences*, 80, 7161-7172.
- [22] Ahoussi K., Koffi Y., Kouassi A., Soro G. and Biemi J., (2013). Étude hydrochimique et microbiologique des eaux de source de l'ouest montagneux de la Côte d'Ivoire: cas du village de Mangouin-Yrongouin (Sous prefecture de Biankouman). [Hydrochemical and microbiological study of water source in the west mountainous of Ivory Coast: case of the village of Mangouin-Yrongouin (Sub-prefecture of Biankouman)]. *Journal of Applied Biosciences*, 63, 4703-4719.
- [23] Safege, (1991). Ville de Pointe Noire, alimentation en eau, réhabilitation des forages, étude de la nappe. [City of Pointe Noire, water supply, rehabilitation of boreholes, study of the water table. Synthesis report, 103 p]. Rapport de synthèse, 103 p.